

**An Experimental and Theoretical Charge Density Study of Theophylline and Malonic Acid Cocrystallization.**

**Bryson A. Hawkins,<sup>1</sup> Jonathan J. Du,<sup>1</sup> Felcia Lai,<sup>1</sup> Stephen A. Stanton,<sup>1</sup> Peter A. Williams,<sup>1,2</sup> Paul W. Groundwater,<sup>1</sup> James A. Platts,<sup>3</sup> Jacob Overgaard<sup>4</sup> and David E. Hibbs<sup>1\*</sup>**

<sup>1</sup>*School of Pharmacy, Faculty of Medicine and Health, The University of Sydney, NSW 2006 Australia*

<sup>2</sup>*School of Science and Health, Western Sydney University, Locked Bag 1797, Penrith, NSW 27513*

<sup>3</sup>*School of Chemistry, Cardiff University, Cardiff, CF10 3AT, UK*

<sup>4</sup>*Department of Chemistry, Center for Materials Crystallography, Aarhus University, Langelandsgade 140, Aarhus C, DK-8000, Denmark*

\*Corresponding author: David E. Hibbs, david.hibbs@sydney.edu.au

†*Electronic supplementary information (ESI) available. CCDC 2119968-2119969 and 2106513 for THEO, MA and (1). For ESI and crystallographic data in CIF or other electronic formats, see DOI: XXXXXXXX*

## Experimental Collection Details

### **Crystal Growth:**

THEO and MA were purchased from Merck (Castle Hill, NSW, Australia) and used without further purification. Single crystals of THEO and MA, were obtained by slow evaporation from dry ethanol. Single crystals of (1) were prepared *via* slow evaporation using the method of Trask *et al.*, by combining equimolar amounts of THEO and MA in a mixture of chloroform and methanol (20 : 1), heating was used to aid dissolution.<sup>1</sup> The solution was allowed to cool and evaporate at room temperature.

### **Data Collection:**

The High-Resolution X-Ray diffraction experiment was performed at the Sydney School of Pharmacy, Faculty of Medicine and Health, University of Sydney, NSW, Australia. The diffraction was performed on an Agilent SuperNova™ Dual Source System with a CCD Atlas detector. A crystal sized 0.82 x 0.43 x 0.25 mm of THEO was mounted on a thin glass fibre with multipurpose Paratone-N, acting as a cryoprotectant and adhesive throughout the collection. Data was collected using a 1°  $\omega$ -scans with the detector distance fixed at 5.3 cm, reciprocal space was covered by positioning the detector arm between 3.47(0) and 52.15(0) ° in 2 $\theta$  with a total of 54614 reflection collected. For MA, a crystal sized 0.36 x 0.62 x 0.74 mm of was mounted on a thin glass fibre with multipurpose Paratone-N, acting as a cryoprotectant and adhesive throughout the collection. Data was collected using a 1°  $\omega$ -scans with the detector distance fixed at 5.3 cm, reciprocal space was covered by positioning the detector arm between 4.04(0) and 65.46(0) ° in 2 $\theta$  with a total of 103698 reflection collected

X-Ray synchrotron data was collected on the BL02B1 beamline at the SPring8 synchrotron in Japan. Data was collected to a resolution of  $(\sin \theta / \lambda)_{\max} = 1.00 \text{ \AA}$  at 20 K using a single crystal with dimension  $0.10 \times 0.09 \times 0.08 \text{ mm}$  at the wavelength of  $0.30988 \text{ \AA}$ . At the time of data collection, the BL02B1 beamline was equipped with a Rigaku kappa goniometer and a cylindrical image-plate detector. Integration of Bragg reflections and subsequent Lorentz–polarization corrections were carried out with the Rigaku RAPID-AUTO software (Rigaku Corp) before further data reduction was performed (see below).

### **Data Reduction and Refinement methods.**

After collection, the data was sorted, scaled and merged using SORTAV by Blessing.<sup>2</sup> The final completenesses for THEO, MA and (1) were, 99.6%, 100% and 97.9%, respectively. The structures of THEO, MA and (1) were solved using direct methods (SHELXT), and a full-matrix least-squares refinement based on  $F^2$  was performed using SHELXL-2015.<sup>3</sup> All X-H covalent bonds were fixed at lengths of 1.009 (N-H), 1.015 (COO-H), 1.059 ( $C_{sp^3}$ -H) and 1.083  $\text{\AA}$  ( $C_{ar}$ -H) based on average values obtained from Allen *et al.* to allow accurate modelling of the EDD.<sup>4</sup> The atomic coordinates and anisotropic temperature factors of the IAM models were imported into the XD program, where a least-squares refinement based on a rigid pseudo-atomic model was performed on  $F$ .<sup>5</sup> XD utilises the Hansen-Coppens multipole formalism to describe the electron density,  $\rho(r)$ , within a crystal system by the summation of the electron density of each aspherical pseudo-atom with nuclear positions  $r_j$  as shown in Equation 1.

$$\rho(r) = \sum_j \rho_j(r - R_j) \quad (1)$$

The complete density of the pseudo-atomic model is described by Equation 2.

$$\rho_j(r_j) = P_c \rho_c + \kappa'^3 P_v \rho_v(\kappa' r) + \kappa''^3 \sum_{l=0}^{l_{max}} R_l(\kappa'' r_j) \sum_{m=0}^{m=l} P_{lm\pm} d_{lm\pm}(\theta, \phi) \quad (2)$$

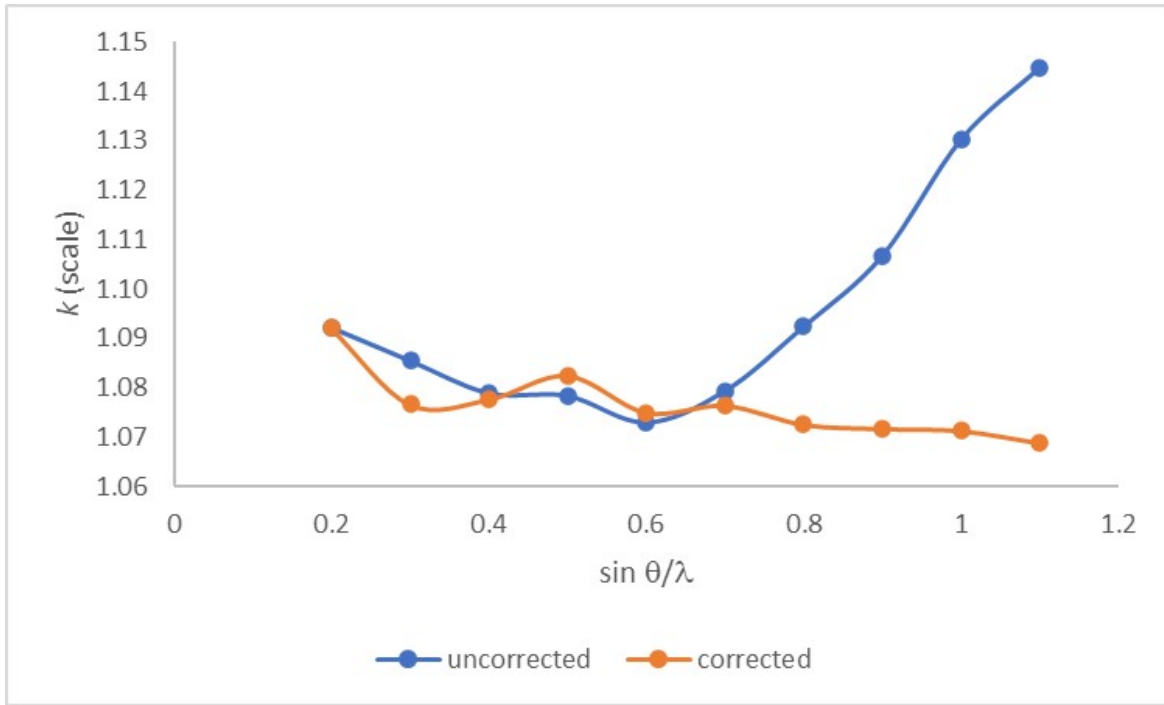
Equation 2 describes a complete pseudo-atomic density, including the spherical core, the valence density, plus a term to describe the aspherical deformation of the valence density. The radial functions  $\{R_l(r_j)\}$  are modulated by angular functions  $\{d_{lm\pm}(\theta, \phi)\}$  defined by local coordinate axes for each atom. A variety of radial functions may be used with the most common being the Slater-type functions expressed in Equation 3.

$$R_l(r) = N r^{n(l)} \exp(-\zeta_l r) \quad (3)$$

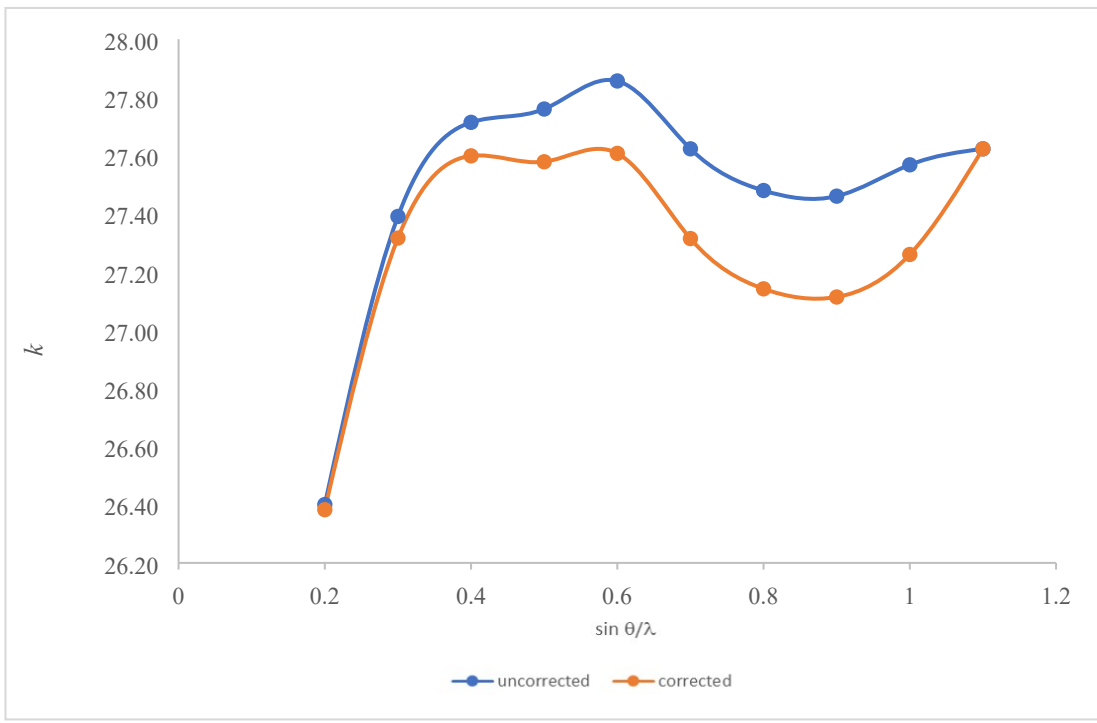
The multipole refinement process began with a high-order spherical atom refinement (usually  $\sin \theta/\lambda > 0.7 \text{ \AA}^{-1}$ ), providing the most accurate atomic positions and temperature factors, which serve as the base for the multipolar model (MM). The atomic multipoles were refined in a stepwise process, the multipoles were truncated at the octapolar level ( $l_{max}=3$ ) for C, O, and N which were also assigned a  $\kappa'$  value (a scalar value governing the expansion and contraction of the spherical valence shell) within the refinement. A single common monopole was used for the H atoms with  $\kappa'$  fixed at a value of 1.2, and the aspherical density modelled by a single bond-directed dipole. The refinement proceeded until convergence for each multipole expansion before further expansion to the successional multipole (*i.e.* Monopole → Dipole...). The atomic positions and temperature factors were refined independently from the multipole expansion model, except for the final refinement cycles where the full variance-covariance matrix is required for standard uncertainties to be meaningful. The refinement was performed using all reflections.

The Hirshfeld rigid bond test investigates the accuracy of the anisotropic displacement parameters (ADPs) obtained in the refinement. Differences in mean-square displacement amplitudes (DMSDA) below  $1 \cdot 10^{-3} \text{ \AA}^2$  indicate a successful deconvolution of the atomic vibrations from the electron density.<sup>6</sup> The maximum observed DMSDA were,  $1.8 \cdot 10^{-3}$ ,  $1.3 \cdot 10^{-3}$   $2.7 \cdot 10^{-3}$  and  $1.3 \cdot 10^{-3} \text{ \AA}^2$  for THEO, MA and (**1**), respectively.

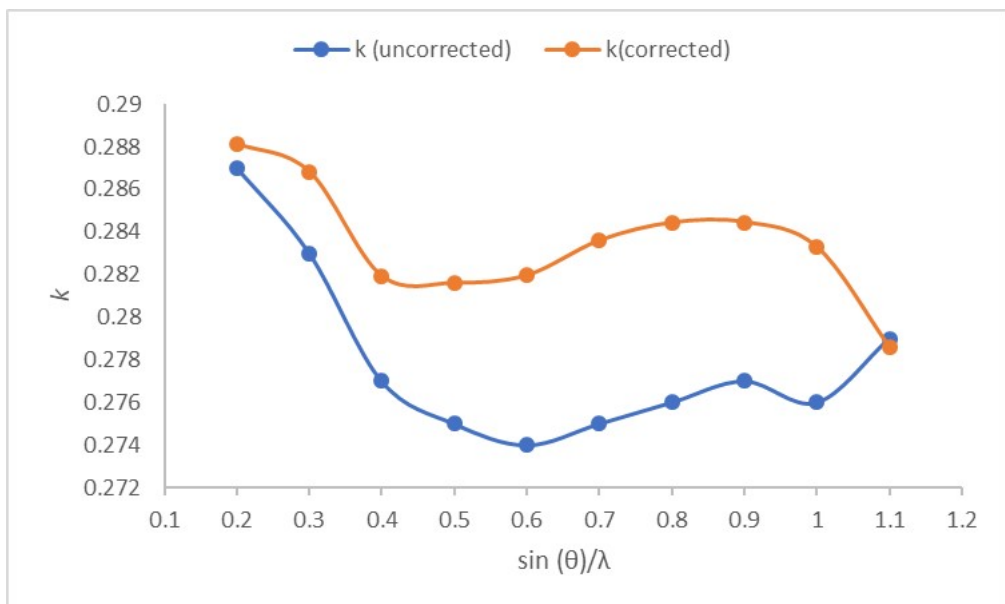
A form of inelastic scattering occurs with phonon absorption and emission; this is known as thermal diffuse scattering (TDS).<sup>7</sup> TDS is structured in reciprocal space, and have maxima, which coincide with Bragg peaks and as such can have a subtle resolution-dependent effect on the integrated intensities, even when the crystal is cooled below 100 K. These errors will primarily affect the ADPs and can also cause significant issues in modelling the EDD.<sup>8</sup> Niepötter *et al.* suggested a method for examining and correcting data for TDS contamination.<sup>8</sup> The correction is achieved by refinement of a number of resolution dependent scale factors, and subsequent fitting of these with a correction factor  $\alpha = a[\frac{\sin(\theta)}{\lambda}]^2 + b[\frac{\sin(\theta)}{\lambda}]^3$ . In THEO, MA and (**1**) the optimal coefficients were found to be  $a = 0.05$ ,  $-0.15$  and  $0.05$  and  $b = 0.5$ ,  $-0.05$  and  $0.7$ , respectively.<sup>8</sup> Figure S1 shows the variation in the resolution dependent scale factors before and after the correction. Residual density analysis using jnk2RDA was carried out after the final model was obtained. The TDS corrected model fitted the data well as shown in the fractal plot of the TDS corrected data post correction, the symmetrical curve indicates the TDS correction decreased the integration error of the intensities due to temperature and resolution errors, and any residual density remaining is likely to be caused by random noise alone.<sup>9</sup>



(a)



(b)



(c)

Figure S1: Resolution dependence of the scale factors for all crystals studied a=THEO, b=MA, c=(1). All scale factors were normalised at their minimum.

Modelling charge density with isotropic temperature factors for hydrogen atoms has been noted to be unsatisfactory by Madsen *et al.* leading to discrepancies in  $\rho$  and  $\nabla^2\rho$  at the bond critical point when compared to combined neutron and X-ray diffraction data.<sup>10</sup> As such, performing a MM refinement using anisotropic temperature factors (ADPs) for the hydrogen atoms is recommended in order to obtain more accurate modelling of the EDD. Anisotropic temperature factors for the hydrogen atoms were calculated using the SHADE3 server, the resultant ADPs generated by the thermal harmonic temperature analysis (THMA-11).<sup>10-12</sup> This MM refinement was carried out as described above; however, the hydrogen temperature factors were not refined because they were fixed at the calculated ADPs.

Using the above methods a total of four MMs were performed on the following data. 1. Normal (no anisotropic temperature factors applied to hydrogen atoms and no correction of TDS). 2. SHADE (anisotropic temperature factors applied to hydrogen atoms and no correction of TDS) 3. TDS (A normal refinement as described in 1. but with TDS corrected data) and 4. TDS + SHADE (A SHADE refinement as described in 2. but with TDS corrected data).

The final model selected for further analysis was the combined the TDS correction with ADPs for all atoms (TDS + SHADE). There were no significant differences in the refinement results or subsequent topological analysis, other than estimation of hydrogen bond energies where the TDS+SHADE MM had better agreement with the theoretical model, specifically with hydrogen bond donor/acceptor to critical point distance. As such, the alternative MMs do not warrant further comparison amongst themselves, and the remainder of the paper will focus on the combined TDS+SHADE MM (the MM results for the other models can be found in ESI and selected crystallographic information can be found below).

Table S1: Calculated hydrogen anisotropic displacement parameters for THEO

<b>Atom</b>	<b>U11</b>	<b>U22</b>	<b>U33</b>	<b>U12</b>	<b>U13</b>	<b>U23</b>
H(6A)	0.0757	0.0406	0.0326	0.0059	0.0163	0.0033
H(6B)	0.0493	0.0580	0.0515	0.0208	0.0177	-0.0099
H(6C)	0.0595	0.0463	0.0421	-0.0109	0.0101	-0.0159
H(1A)	0.0277	0.0474	0.0241	0.0094	0.0035	-0.0097
H(7A)	0.0480	0.0490	0.0653	0.0013	-0.0166	0.0209
H(7B)	0.0275	0.0757	0.0659	0.0141	-0.0014	0.0035
H(7C)	0.0461	0.0545	0.0613	0.0010	-0.0238	-0.0069
H(1)	0.0248	0.0584	0.0368	0.0138	-0.0083	-0.0065

Table S3: Calculated hydrogen anisotropic displacement parameters for MA

<b>Atom</b>	<b>U11</b>	<b>U22</b>	<b>U33</b>	<b>U12</b>	<b>U13</b>	<b>U23</b>
H(04)	0.0343	0.0220	0.0458	0.0011	0.0153	-0.0040
H(01)	0.0514	0.0430	0.0271	0.0151	0.0190	0.0042
H(02A)	0.0267	0.0469	0.0414	0.0146	-0.0049	0.0002
H(02B)	0.0524	0.0287	0.0460	-0.0026	0.0304	0.0078

Table S4: Calculated hydrogen anisotropic displacement parameters for (**1**)

<b>Atom</b>	<b>U11</b>	<b>U22</b>	<b>U33</b>	<b>U12</b>	<b>U13</b>	<b>U23</b>
H(1)	0.01365	0.01183	0.02654	0.00667	0.00505	0.01365
H(1A)	0.04718	0.0222	0.0181	0.01683	0.01326	-0.00603
H(6A)	0.01989	0.01271	0.03399	0.00141	-0.00436	0.00839
H(6B)	0.03444	0.00738	0.0428	0.0166	0.0163	0.01403
H(6C)	0.02431	0.01812	1932	-0.00609	0.00261	0.0077
H(7A)	0.04498	0.02836	0.02442	0.01036	0.03044	0.00492
H(7B)	0.02109	0.03105	0.00729	0.016	0.00033	-0.0039
H(7C)	0.02644	0.0212	0.014	0.007	0.009	-0.00473
H(01)	0.06816	0.02345	0.04738	-0.0092	0.01846	-0.00003
H(02A)	0.02067	0.02566	0.01727	0.01052	0.012	0.00235
H(02B)	0.04414	0.01581	0.02533	0.01509	0.01739	-0.00109
H(04)	0.03402	0.08534	0.0523	-0.0208	0.0397	-0.00796

Table S5: Atomic coordinates ( $\times 10^4$ ) and equivalent isotropic displacement parameters ( $\text{\AA}^2 \times 10^3$ ) for THEO.

	<b>x</b>	<b>y</b>	<b>z</b>	<b>U(eq)</b>
C(1)	7508(1)	3039(3)	5871(1)	18(1)
C(2)	6702(1)	5174(2)	5986(1)	14(1)
C(3)	5814(1)	7357(3)	5383(1)	19(1)
C(4)	6369(1)	4414(2)	3273(1)	15(1)
C(5)	6776(1)	4022(2)	4465(1)	13(1)
C(6)	6157(1)	7895(3)	8111(1)	26(1)
C(7)	5456(1)	6787(4)	2709(2)	31(1)
N(1)	7301(1)	2653(2)	4420(1)	15(1)
N(2)	7156(1)	4570(2)	6878(1)	18(1)
N(3)	6225(1)	6738(2)	6476(1)	18(1)
N(4)	5899(1)	6124(2)	3842(1)	18(1)
O(2)	6412(1)	3438(3)	1890(1)	22(1)
O(1)	5395(1)	8948(3)	5741(2)	32(1)

Table S6: Atomic coordinates ( $\times 10^4$ ) and equivalent isotropic displacement parameters ( $\text{\AA}^2 \times 10^3$ ) for MA.

	x	y	z	U(eq)
O(03)	4561(1)	3075(1)	1249(1)	17(1)
O(04)	8327(1)	1772(1)	522(1)	20(1)
O(01)	7321(1)	7564(1)	5194(1)	28(1)
O(02)	5840(1)	9369(1)	3140(1)	28(1)
C(01)	7164(1)	7855(1)	3651(1)	15(1)
C(03)	6981(1)	3485(1)	1365(1)	13(1)
C(02)	8736(1)	6104(1)	2532(1)	16(1)

Table S3: Atomic coordinates ( $\times 10^4$ ) and equivalent isotropic displacement parameters ( $\text{\AA}^2 \times 10^3$ ) for (1). U(eq) is defined as one third of the trace of the orthogonalized  $U_{ij}$  tensor.

	x	y	z	U(eq)
O(1)	5.55	0.76	10.73	0.009
O(2)	8.80	-2.27	9.60	0.012
N(1)	9.80	-0.14	7.61	0.008
N(2)	8.74	1.82	7.43	0.008
N(3)	7.01	1.39	9.09	0.007
N(4)	7.17	-0.74	10.14	0.007
C(1)	9.76	1.06	7.00	0.009
C(2)	8.12	1.05	8.37	0.007
C(3)	6.52	0.50	10.03	0.007
C(4)	8.30	-1.15	9.42	0.007
C(5)	8.74	-0.16	8.50	0.007
C(6)	6.45	2.73	8.99	0.010
C(7)	6.63	-1.64	11.16	0.010
H(1)	10.39	1.31	6.37	0.014
H(1A)	10.40	-0.70	7.40	0.023
H(6A)	7.05	3.37	9.34	0.024
H(6B)	5.63	2.76	9.48	0.024
H(6C)	6.27	2.92	8.07	0.021
H(7A)	7.10	-2.46	11.00	0.025
H(7B)	5.69	-1.76	11.00	0.018
H(7C)	6.77	-1.27	12.00	0.019

O(01)	10.60	7.51	4.47	0.010
O(02)	10.80	5.63	3.25	0.012
O(03)	10.30	3.82	5.48	0.011
O(04)	8.28	4.17	6.31	0.012
C(01)	10.30	6.29	4.10	0.008
C(02)	9.09	5.81	4.83	0.011
C(03)	9.31	4.51	5.57	0.007
H(01)	11.30	7.73	4.01	0.044
H(02A)	8.40	5.61	4.14	0.020
H(02B)	8.70	6.47	5.43	0.025
H(04)	8.39	3.35	6.74	0.044

---

Table S7: Bond Lengths ( $\text{\AA}$ ) and Angles ( $^\circ$ ) of THEO

C(1)-N(1)	1.3378(10)
C(1)-N(2)	1.3416(11)
C(1)-H(1)	1.03(2)
C(2)-N(2)	1.3594(11)
C(2)-N(3)	1.3680(10)
C(2)-C(5)	1.3738(10)
C(3)-O(1)	1.2221(12)
C(3)-N(3)	1.3850(14)
C(3)-N(4)	1.4025(14)
C(4)-O(2)	1.2333(11)
C(4)-N(4)	1.3994(11)
C(4)-C(5)	1.4251(10)
C(5)-N(1)	1.3789(10)
C(6)-N(3)	1.4634(13)
C(6)-H(6A)	0.98(2)
C(6)-H(6B)	1.01(2)
C(6)-H(6C)	1.01(2)
C(7)-N(4)	1.4677(14)
C(7)-H(7A)	1.00(2)
C(7)-H(7B)	0.98(2)
C(7)-H(7C)	0.99(2)
N(1)-H(1A)	0.98(2)
N(1)-C(1)-N(2)	113.00(7)
N(1)-C(1)-H(1)	118.0(17)
N(2)-C(1)-H(1)	129.0(17)
N(2)-C(2)-N(3)	126.54(7)
N(2)-C(2)-C(5)	111.21(6)

N(3)-C(2)-C(5)	122.25(7)
O(1)-C(3)-N(3)	121.41(11)
O(1)-C(3)-N(4)	121.24(11)
N(3)-C(3)-N(4)	117.35(7)
O(2)-C(4)-N(4)	122.41(8)
O(2)-C(4)-C(5)	125.71(8)
N(4)-C(4)-C(5)	111.88(7)
C(2)-C(5)-N(1)	105.48(6)
C(2)-C(5)-C(4)	122.78(7)
N(1)-C(5)-C(4)	131.72(7)
N(3)-C(6)-H(6A)	111(2)
N(3)-C(6)-H(6B)	110(3)
H(6A)-C(6)-H(6B)	110(3)
N(3)-C(6)-H(6C)	109(2)
H(6A)-C(6)-H(6C)	115(3)
H(6B)-C(6)-H(6C)	101(3)
N(4)-C(7)-H(7A)	108(2)
N(4)-C(7)-H(7B)	112(3)
H(7A)-C(7)-H(7B)	98(4)
N(4)-C(7)-H(7C)	106(2)
H(7A)-C(7)-H(7C)	122(3)
H(7B)-C(7)-H(7C)	111(4)
C(1)-N(1)-C(5)	106.50(6)
C(1)-N(1)-H(1A)	124.3(19)
C(5)-N(1)-H(1A)	129.1(18)
C(1)-N(2)-C(2)	103.82(6)
C(2)-N(3)-C(3)	119.01(8)
C(2)-N(3)-C(6)	120.81(9)
C(3)-N(3)-C(6)	120.12(9)
C(4)-N(4)-C(3)	126.62(7)
C(4)-N(4)-C(7)	117.00(10)
C(3)-N(4)-C(7)	116.35(9)

---

Table S8: Bond Lengths ( $\text{\AA}$ ) and Angles ( $^\circ$ ) of MA

O(03)-C(03)	1.2259(5)
O(04)-C(03)	1.3048(5)
O(04)-H(04)	0.945(11)
O(01)-C(01)	1.3090(6)
O(01)-H(01)	0.924(13)
O(02)-C(01)	1.2207(6)
C(01)-C(02)	1.5044(6)
C(03)-C(02)	1.5099(6)
C(02)-H(02A)	1.095(2)
C(02)-H(02B)	1.095(2)

C(03)-O(04)-H(04)	110.2(8)
C(01)-O(01)-H(01)	109.5(10)
O(02)-C(01)-O(01)	123.71(4)
O(02)-C(01)-C(02)	122.52(4)
O(01)-C(01)-C(02)	113.76(4)
O(03)-C(03)-O(04)	125.10(4)
O(03)-C(03)-C(02)	122.37(4)
O(04)-C(03)-C(02)	112.52(4)
C(01)-C(02)-C(03)	110.20(3)
C(01)-C(02)-H(02A)	110.9(6)
C(03)-C(02)-H(02A)	107.9(6)
C(01)-C(02)-H(02B)	108.3(6)
C(03)-C(02)-H(02B)	107.1(6)
H(02A)-C(02)-H(02B)	112.4(9)

---

Table S9: Table S4: Bond Lengths ( $\text{\AA}$ ) and Angles ( $^\circ$ ) of **(1)**

O(1)-C(3)	1.2217
O(2)-C(4)	1.2351
N(1)-C(1)	1.3406
N(1)-C(5)	1.3795
N(2)-C(1)	1.3438
N(2)-C(2)	1.3612
N(3)-C(2)	1.3664
N(3)-C(3)	1.3817
N(3)-C(6)	1.4616
N(4)-C(3)	1.405
N(4)-C(4)	1.3994
N(4)-C(7)	1.4713
C(2)-C(5)	1.3728
C(4)-C(5)	1.4197
O(01)-C(01)	1.3268
O(02)-C(01)	1.2132
O(03)-C(03)	1.2206
O(04)-C(03)	1.3153
C(01)-C(02)	1.5051
C(02)-C(03)	1.5104

C(1)	N(1)	C(5)	106.85(3)
C(1)	N(1)	H(1A)	126.1(7)
C(5)	N(1)	H(1A)	127.0(7)

C(1)	N(2)	C(2)	104.31(3)
C(2)	N(3)	C(3)	119.45(3)
C(2)	N(3)	C(6)	120.02(3)
C(3)	N(3)	C(6)	120.15(3)
C(3)	N(4)	C(4)	126.35(3)
C(3)	N(4)	C(7)	115.14(3)
C(4)	N(4)	C(7)	118.46(3)
N(1)	C(1)	N(2)	112.35(4)
N(1)	C(1)	H(1)	122.1(6)
N(2)	C(1)	H(1)	125.5(6)
N(2)	C(2)	N(3)	126.67(3)
N(2)	C(2)	C(5)	110.96(3)
N(3)	C(2)	C(5)	122.37(3)
O(1)	C(3)	N(3)	122.32(4)
O(1)	C(3)	N(4)	120.69(4)
N(3)	C(3)	N(4)	116.99(3)
O(2)	C(4)	N(4)	121.14(4)
O(2)	C(4)	C(5)	126.36(4)
N(4)	C(4)	C(5)	112.50(3)
N(1)	C(5)	C(2)	105.54(3)
N(1)	C(5)	C(4)	132.16(3)
C(2)	C(5)	C(4)	122.31(3)
N(3)	C(6)	H(6A)	109.8(6)
N(3)	C(6)	H(6B)	108.7(6)
N(3)	C(6)	H(6C)	108.8(6)
H(6A)	C(6)	H(6B)	109.4(9)
H(6A)	C(6)	H(6C)	110.1(9)
H(6B)	C(6)	H(6C)	110.0(9)
N(4)	C(7)	H(7A)	106.4(7)
N(4)	C(7)	H(7B)	109.3(6)
N(4)	C(7)	H(7C)	110.6(6)
H(7A)	C(7)	H(7B)	111.5(9)
H(7A)	C(7)	H(7C)	109.9(9)
H(7B)	C(7)	H(7C)	109.1(9)
C(01)	O(01)	H(01)	108.3(9)
C(03)	O(04)	H(04)	113.1(8)
O(01)	C(01)	O(02)	124.35(4)
O(01)	C(01)	C(02)	112.96(3)
O(02)	C(01)	C(02)	122.66(4)
C(01)	C(02)	C(03)	112.92(4)
C(01)	C(02)	H(02A)	105.6(6)
C(01)	C(02)	H(02B)	111.4(6)
C(03)	C(02)	H(02A)	105.7(6)

C(03)	C(02)	H(02B)	110.2(6)
H(02A)	C(02)	H(02B)	110.6(9)
O(03)	C(03)	O(04)	122.88(4)
O(03)	C(03)	C(02)	124.84(4)
O(04)	C(03)	C(02)	112.27(3)

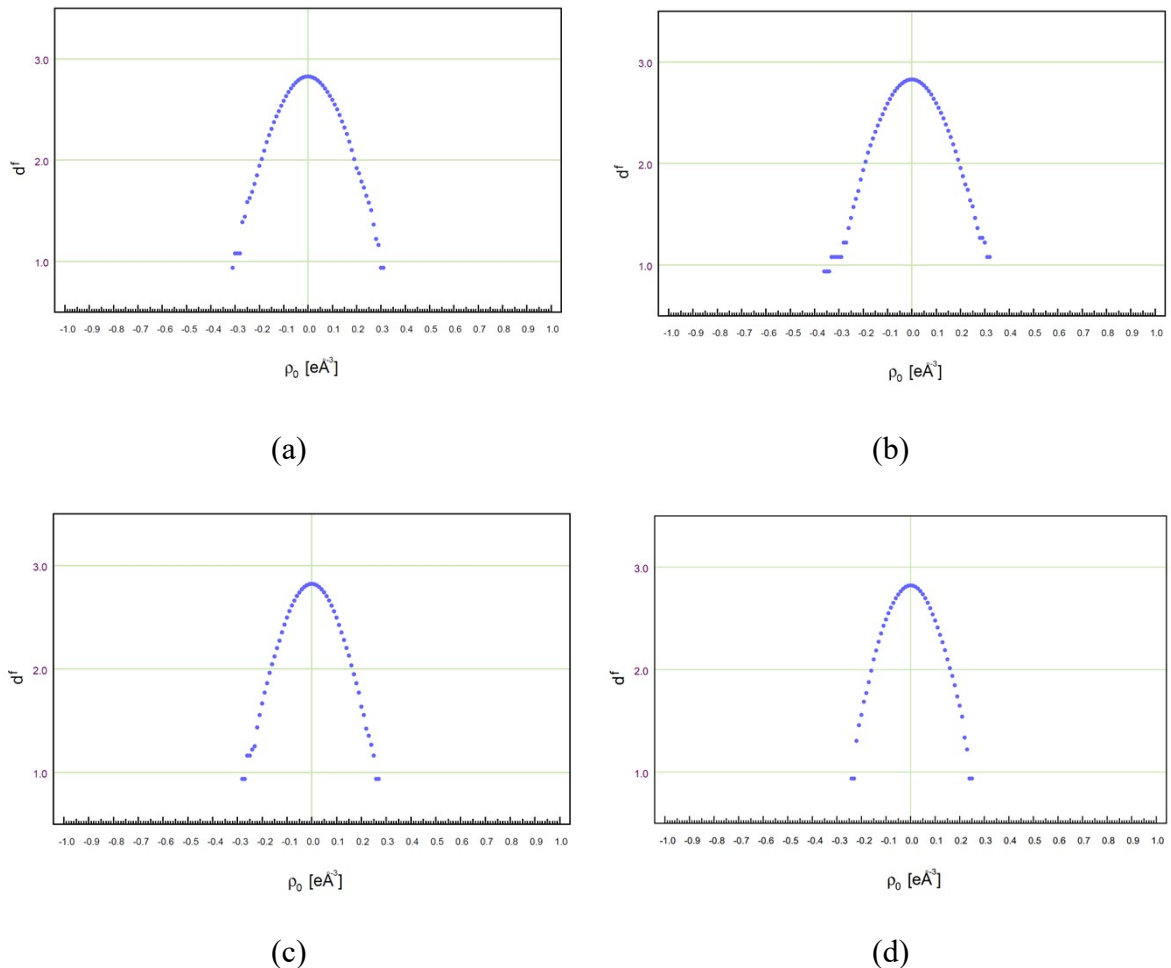
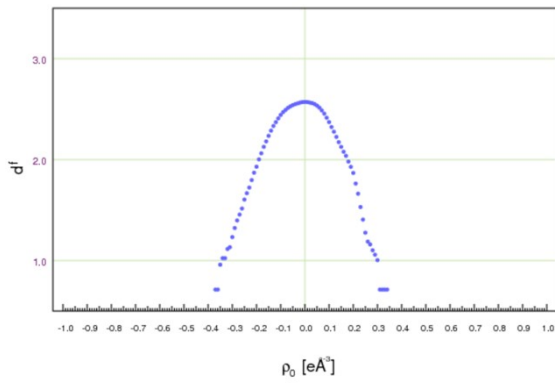
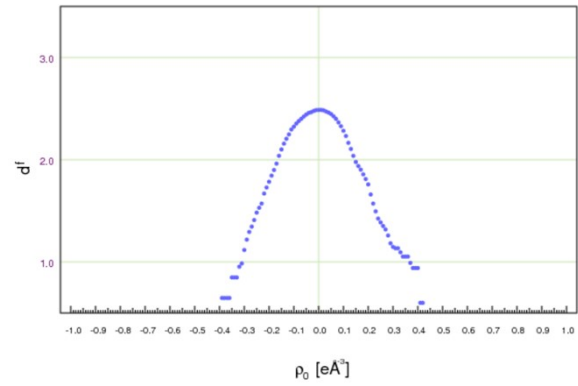


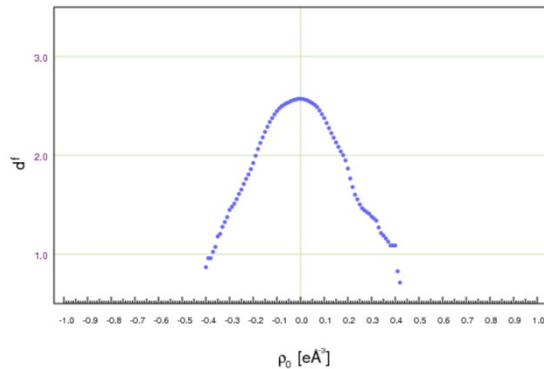
**Figure S2:** fractal plot for THEO; residual density vs. fractal dimension (a) Normal, (b) TDS, (c) SHADE, (d) SHADE+TDS



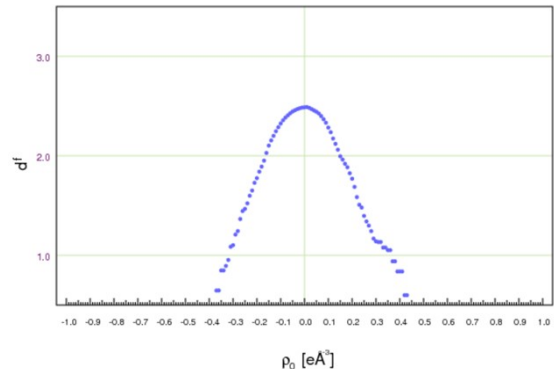
(a)



(b)

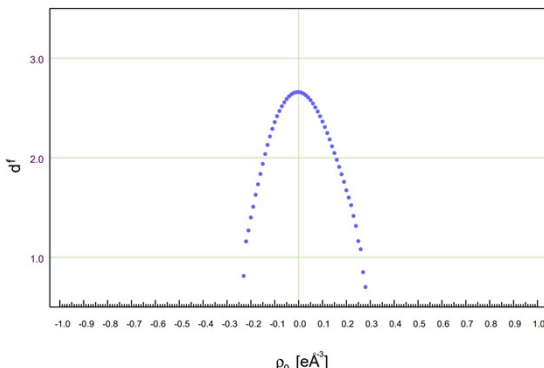


(c)

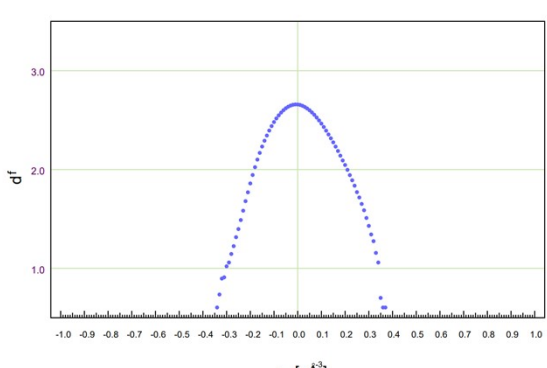


(d)

**Figure S3:** fractal plot for MA; residual density vs. fractal dimension (a) Normal, (b) TDS, (c) SHADE, (d) SHADE+TDS



(a)



(b)

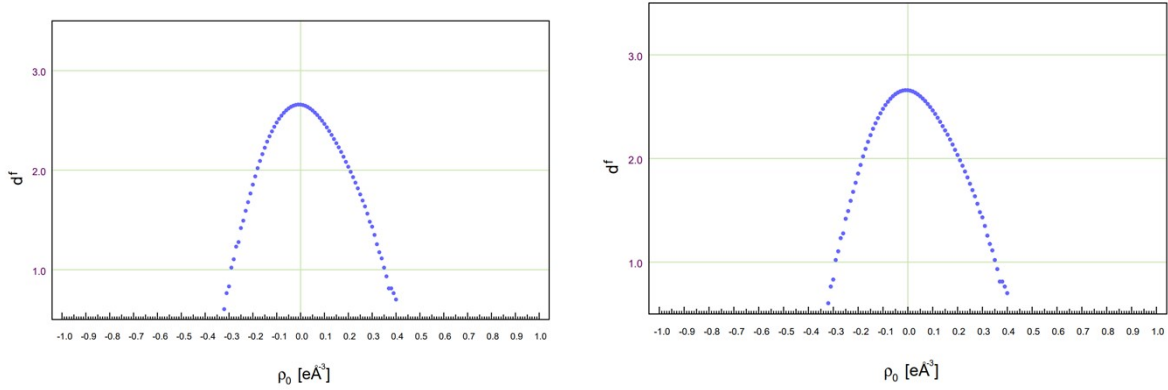


**Figure S4:** fractal plot for (1); residual density vs. fractal dimension (a) Normal, (b) TDS, (c) SHADE, (d) SHADE+TDS

## Topological Analysis

**Table S9:** List of bond critical points (BCP's) found from topological analysis of experimental and theoretical models for MM of THEO.

	NORMAL		SHADE		TDS		SHADE+TDS		SP				
	$\rho$ ( $e\text{\AA}^{-3}$ )	$\nabla^2\rho$ ( $e\text{\AA}^{-5}$ )	$\varepsilon$	$\rho$ ( $e\text{\AA}^{-3}$ )	$\nabla^2\rho$ ( $e\text{\AA}^{-5}$ )	$\varepsilon$	$\rho$ ( $e\text{\AA}^{-3}$ )	$\nabla^2\rho$ ( $e\text{\AA}^{-5}$ )	$\varepsilon$	$\rho$ ( $e\text{\AA}^{-3}$ )	$\nabla^2\rho$ ( $e\text{\AA}^{-5}$ )	$\varepsilon$	
O(1) - C(3)	2.84 9	- 21.417	0. 09	2.87 3	- 16.929	0. 1	2.83 5	- 23.95 6	0. 12	2.801 11.95 6	- 0. 1	2.7830 64 4.552 65	0.124 324
O(2) - C(4)	2.83 3	-8.856	0. 07	2.77 7	-2.899	0. 07	2.80 2	- 13.27	0. 11	2.797 1.429	- 0. 03	2.7005 31 5.562 31	0.101 615
N(1) - C(1)	2.43 4	- 25.563	0. 16	2.37 1	- 23.743	0. 21	2.37 4	- 28.34 6	0. 2	2.336 21.70 2	- 0. 07	2.2472 12 16.01 68	0.204 343
N(1) - C(5)	2.09 1	- 16.354	0. 09	2.08 4	- 16.655	0. 11	2.05 7	- 16.95 9	0. 09	2.119 22.86 9	- 0. 13	2.0195 49 15.29 84	0.235 51
N(1) - H(1A)	2.03 9	- 34.372	0. 05	1.91 6	- 24.891	0. 05	1.88 4	- 24.56 1	0. 05	1.841 19.50 8	- 0. 01	2.3027 64 45.03 3	0.034 059
N(2) - C(1)	2.51 3	- 21.903	0. 13	2.54 8	- 23.188	0. 16	2.48 7	- 23.17 8	0. 2	2.476 26.29 5	- 0. 23	2.2472 12 16.01 68	0.204 343
N(2) - C(2)	2.29 4	- 17.735	0. 22	2.29 4	- 19.145	0. 18	2.26 8	- 20.38 9	0. 23	2.342 25.64 2	- 0. 24	2.3745 19 29.40 09	0.242 425
N(3) - C(2)	2.19 6	- 19.934	0. 23	2.16 5	- 20.343	0. 2	1.89 8	- 20.47 9	0. 11	2.156 22.49 8	- 0. 12	2.1586 19 24.14 1	0.134 717
N(3) - C(3)	2.14 8	- 21.278	0. 04	2.13 5	- 21.059	0. 01	2.15 7	- 22.49 7	0. 3	2.038 19.78 8	- 0. 07	2.1262 88 25.67 24	0.184 251
N(3) - C(6)	1.84 4	- 12.727	0. 09	1.78 2	- 11.719	0. 08	2.11 1	- 22.98 1	0. 08	1.877 18.89 2	- 0. 09	1.6963 11 15.72 3	0.011 719
C(6) - H(6B)	2.05 3	- 18.873	0. 21	2.06 4	- 18.498	0. 11	1.76 3	- 13.48	0. 04	2.102 24.89	- 0. 07	2.0608 76 29.29	0.039 429

								8			6			4	
N(4) - C(3)	2.09 1	- 19.186	0. 09	2.01 1	- 16.603	0. 11	2.07	- 20.12 6	0. 15	2.011	- 20.90 6	0. 28	2.0522 92	- 23.98 87	0.168 021
N(4) - C(4)	1.96 7	- 15.593	0. 1	1.72 7	- 11.955	0. 14	1.97 1	- 17.96	0. 13	1.72	- 17.03 1	0. 14	2.0448 42	- 23.78 16	0.112 209
N(4) - C(7)	1.72 6	- 16.636	0. 07	1.80 1	- 20.778	0. 08	1.74 2	- 18.46 5	0. 09	1.829	- 23.93 4	0. 01	1.6895 62	- 15.33 65	0.053 483
C(7) - H(7B)	2.16	- 32.446	0. 39	2.28 9	- 22.195	0. 15	2.27 4	- 22.57 1	0. 21	2.276	- 23.99 7	0. 19	2.0668 08	- 29.29 85	0.040 916
C(1) - H(1)	1.94 2	- 20.156	0. 12	2.02 2	- 17.257	0. 22	2.02 6	- 17.09 5	0. 25	2.054	- 19.64 4	0. 23	1.9675	- 27.23 09	0.046 94
C(2) - C(5)	2.28 7	- 21.091	0. 15	1.82 6	- 20.604	0. 23	1.86	- 17.58 8	0. 29	1.872	- 20.82 3	0. 31	2.2436 82	- 22.76 8	0.344 643
C(4) - C(5)	2.01 8	- 16.373	0. 21	1.65 9	- 20.676	0. 12	2.15 2	- 22.78 1	0. 31	1.511	- 10.22 2	0. 31	2.0417 25	- 20.36 99	0.202 075
C(6) - H(6A)	1.84 8	- 18.657	0. 2	1.73 1	- 13.072	0. 39	1.72 5	- 13.20 5	0. 51	1.71	- 13.12 3	0. 35	2.0430 2	- 28.46 62	0.050 227
C(6) - H(6C)	1.76 2	- 13.629	0. 34	1.56 5	- 14.198	0. 44	1.7	- 15.11 4	0. 59	1.396	- 7.866	1. 06	2.0430 2	- 28.46 62	0.050 227
C(7) - H(7A)	1.91 4	- 20.856	0. 42	1.34 1	- 53.919	0. 09	2.16 7	- 25.30 6	0. 74	1.217	- 14.69	0. 47	2.0342 88	- 27.87 47	0.058 493
C(7) - H(7C)	1.61 2	- 13.743	0. 48	1.68	- 13.743	0. 47	1.68	- 16.04	0. 54	1.434	- 5.082	0. 6	2.0470 83	- 29.01 39	0.041 514

Table S10: List of bond critical points (BCP's) found from topological analysis of experimental and theoretical models for MM of MA.

	Normal			SHADE			TDS			SHADE+TDS			SP		
	$\rho$ (e $\text{\AA}^{-3}$ )	$\nabla^2\rho$ (e $\text{\AA}^{-5}$ )	$\epsilon$	$\rho$ (e $\text{\AA}^{-3}$ )	$\nabla^2\rho$ (e $\text{\AA}^{-5}$ )	$\epsilon$	$\rho$ (e $\text{\AA}^{-3}$ )	$\nabla^2\rho$ (e $\text{\AA}^{-5}$ )	$\epsilon$	$\rho$ (e $\text{\AA}^{-3}$ )	$\nabla^2\rho$ (e $\text{\AA}^{-5}$ )	$\epsilon$	$\rho$ (e $\text{\AA}^{-3}$ )	$\nabla^2\rho$ (e $\text{\AA}^{-5}$ )	$\epsilon$

O(03) -C(03)	2.80 3	- 26.50 7	0.2 2	2.84 2	-33.47	0.2 3	2.83 6	- 28.59 3	0.2 2	2.86 9	- 33.35 2	0.2 3	2.22229 7	- 4.4736 3	0.01375 5
O(04) -C(03)	2.35 4	- 24.55 5	0.1 4	2.35 6	- 23.20 6	0.1 9	2.37 1	- 23.52 1	0.1 4	2.36 2	-21.9	0.1 8	2.75097 5	- 3.1074 2	0.12019 4
O(04) -H(04)	1.85 4	- 23.21 1	0 0	1.81 9	- 19.46 4	0.0 1	1.85 4	- 24.31 5	0	1.82 5	- 20.17 5	0.0 1	2.02390 2	- 36.009 3	0.01300 4
O(01) -C(01)	2.33 5	- 21.95 2	0.1 7	2.41 5	- 19.58 9	0.2 3	2.34 7	-20.63	0.1 7	2.42 5	- 18.38 2	0.2 3	2.20225 4	- 5.3507 5	0.01923
O(01) -H(01)	1.91 9	- 16.27 2	0	1.97 4	- 16.94 6	0.0 2	1.93 3	- 16.72 5	0	2	- 17.01 7	0.0 2	2.02254 6	- 36.008 9	0.01247 4
O(02) -C(01)	2.77 1	- 11.80 5	0.2	2.87 9	- 18.11 2	0.6 1	2.80 4	- 14.60 4	0.2	2.88 8	- 16.01 9	0.6 6	2.74764 2	- 3.0569 3	0.12666 3
C(01) -C(02)	1.75 4	- 13.18 1	0.0 6	1.70 3	- 11.33 9	0.1 5	1.75 4	- 12.93 8	0.0 6	1.69 5	- 10.98 7	0.1 5	1.75622 9	- 15.637 8	0.07728 7
C(03) -C(02)	1.65 5	- 11.96 1	0.2	1.68 4	- 10.72 4	0.2	1.65 6	- 11.69 2	0.2	1.68	- 10.40 1	0.2	1.79561 2	- 16.570 2	0.05088 3
C(02) -H(02A)	1.70 7	- 13.74 9	0.0 5	1.76	- 14.02 7	0.0 2	1.71 7	- 13.63 2	0.0 6	1.77 6	- 14.00 3	0.0 3	1.84377 5	- 23.030 5	0.01144
C(02) -H(02B)	1.79 5	- 14.47 8	0.0 6	1.73	- 13.63 8	0.0 2	1.81	- 14.41 9	0.0 5	1.74 6	- 13.44 6	0.0 3	1.84949 1	- 22.955 3	0.01028 9

Table S11: List of bond critical points (BCP's) found from topological analysis of experimental and theoretical models for MM of (1).

NORMAL		SHADE			SHADE +TDS			TDS				
$\rho(\text{e}\text{\AA}^{-3})$	$\nabla^2\rho(\text{e}\text{\AA}^{-5})$	$\varepsilon$	$\rho(\text{e}\text{\AA}^{-3})$									
3.157( 29)	44.352(157)	0.18	3.156( 29)	44.040(158)	0.17	3.063( 25)	42.684(148)	0.17	3.063( 37)	42.780(212)	0.17	2.70
-	-	-	-	-	-	-	-	-	2.817( -37)	-	-	2.73
2.878( 28)	36.684(153)	0.12	2.883( 28)	36.840(154)	0.11	2.809( 24)	35.530(140)	0.1	35.882(203)	0.09	-	0.09
-	-	-	-	-	-	-	-	-	2.213( -36)	-	-	2.04
2.293( 26)	23.724(121)	0.11	2.283( 27)	23.616(123)	0.12	2.219( 23)	24.265(112)	0.1	24.407(154)	0.1	-	0.1
-	-	-	-	-	-	-	-	-	1.853( -31)	-	-	2.34
1.867( 37)	30.560(264)	0.01	1.919( 35)	30.413(243)	0.01	1.849( 28)	26.591(199)	0.01	26.765(201)	0.01	-	0.01
-	-	-	-	-	-	-	-	-	3.033( -28)	-	-	2.77
3.132( 31)	42.193(174)	0.15	3.126( 31)	42.136(176)	0.15	3.036( 27)	40.184(160)	0.14	40.255(227)	0.14	-	0.14
-	-	-	-	-	-	-	-	-	2.911( -38)	35.633(219)	0.12	2.76
3.014( 30)	40.219(168)	0.14	3.008( 30)	40.217(170)	0.14	2.916( 26)	35.729(156)	0.12	2.340( -30)	-	-	2.06
-	-	-	-	-	-	-	-	-	26.257(146)	0.12	-	-
2.407( 25)	25.770(114)	0.15	2.392( 26)	25.867(117)	0.15	2.356( 21)	26.115(103)	0.12	1.850( -30)	-	-	2.17
-	-	-	-	-	-	-	-	-	-	-	-	-
1.656( 32)	20.585(245)	0.01	1.882( 41)	20.519(258)	0.01	1.693( 26)	16.979(187)	0.01	16.733(222)	0.01	-	0.01
-23.688(	-	-	-	-23.675(	-	-	-25.535(	-	2.301( -34)	-	-	2.08
2.347( 25)	98)	0.2	2.345( 25)	99)	0.22	2.300( 21)	90)	0.2	25.671(122)	0.22	-	0.22
-17.551(	-	-	-	-17.435(	-	-	-18.582(	-	2.115( -27)	-18.518(	-	2.07
2.146( 23)	82)	0.23	2.137( 23)	83)	0.23	2.118( 19)	71)	0.23	97)	0.23	-	0.23
-	-	-	-	-	-	-	-	-	2.083( -25)	-	-	2.25
2.010( 37)	27.530(243)	0.05	2.162( 38)	27.528(216)	0.05	1.963( 28)	25.561(187)	0.05	25.681(184)	0.05	-	0.05
-21.148(	-	-	-	-21.025(	-	-	-22.145(	-	2.392( -24)	-22.066(	-	2.40
2.416( 22)	77)	0.17	2.418( 22)	77)	0.18	2.389( 18)	66)	0.18	91)	0.18	-	0.18
-18.274(	-	-	-	-18.112(	-	-	-18.706(	-	2.273( -24)	-18.605(	-	2.20
2.298( 21)	73)	0.17	2.292( 21)	73)	0.16	2.277( 17)	60)	0.16	83)	0.15	-	0.15
-	-	-	-	-	-	-	-	-	0.359( -23)	-	-	0.38
0.317( 24)	4.468( 40)	0.06	0.316( 29)	5.258( 45)	0.07	0.352( 19)	4.223( 29)	0.06	4.681( 36)	0.06	-	0.06
-20.845(	-	-	-	-20.701(	-	-	-22.244(	-	2.236( -24)	-22.186(	-	2.10
2.259( 22)	83)	0.24	2.251( 22)	83)	0.24	2.239( 18)	72)	0.22	99)	0.23	-	0.23
-21.349(	-	-	-	-21.333(	-	-	-21.799(	-	2.173( -23)	-21.891(	-	2.03
2.197( 22)	78)	0.27	2.194( 22)	79)	0.27	2.172( 18)	66)	0.25	90)	0.25	-	0.25
-10.018(	-	-	-	-10.174(	-	-	-11.114(	-	1.694( -22)	-11.245(	-	1.71
1.713( 23)	68)	0.08	1.714( 22)	68)	0.08	1.692( 19)	58)	0.08	74)	0.08	-	0.08
-18.072(	-	-	-	-17.888(	-	-	-18.577(	-	2.056( -21)	-18.455(	-	1.98
2.068( 20)	70)	0.24	2.064( 20)	70)	0.24	2.056( 16)	59)	0.22	79)	0.21	-	0.21
-17.811(	-	-	-	-17.746(	-	-	-18.362(	-	2.088( -22)	-18.280(	-	2.02
2.104( 21)	72)	0.2	2.101( 21)	73)	0.19	2.085( 17)	62)	0.18	84)	0.18	-	0.18
-11.056(	-	-	-	-11.330(	-	-	-11.790(	-	1.686( -22)	-11.991(	-	1.72
1.694( 23)	69)	0.06	1.692( 23)	69)	0.07	1.689( 19)	58)	0.05	74)	0.06	-	0.06
-	-	-	-	-	-	-	-	-	1.894( -26)	-19.904(	-	1.94
1.842( 34)	19.840(142)	0.1	1.961( 33)	20.752(113)	0.12	1.811( 26)	19.131(112)	0.1	94)	0.11	-	0.11
-20.738(	-	-	-	-20.604(	-	-	-21.313(	-	2.211( -22)	-21.293(	-	2.27
2.217( 20)	56)	0.29	2.210( 20)	56)	0.29	2.215( 16)	45)	0.29	66)	0.29	-	0.29
-18.319(	-	-	-	-18.208(	-	-	-18.579(	-	2.049( -21)	-18.589(	-	2.05
2.046( 19)	50)	0.3	2.042( 19)	50)	0.3	2.048( 15)	39)	0.28	58)	0.28	-	0.28
-	-	-	-	-15.093(	-	-	-15.333(	-	1.771( -21)	-14.689(	-	1.87
1.850( 37)	15.384(106)	0.15	1.818( 32)	96)	0.13	1.820( 28)	81)	0.15	79)	0.13	-	0.13
-	-	-	-	-	-	-	-	-	1.862( -26)	-17.947(	-	1.89
1.896( 41)	18.154(134)	0.13	1.911( 35)	18.285(104)	0.14	1.860( 31)	17.981(102)	0.13	83)	0.14	-	0.14
-	-	-	-	-17.329(	-	-	-15.869(	-	1.852( -27)	-16.971(	-	1.88
1.836( 34)	15.952(102)	0.13	1.912( 32)	83)	0.15	1.800( 26)	77)	0.13	69)	0.15	-	0.15
-	-	-	-	-19.999(	-	-	-17.563(	-	1.879( -25)	-18.863(	-	1.89
1.823( 37)	18.203(107)	0.11	1.923( 33)	84)	0.13	1.814( 28)	82)	0.1	72)	0.12	-	0.12
-	-	-	-	-	-	-	-	-	1.704( -27)	-14.868(	-	1.88
1.812( 37)	16.018(124)	0.11	1.739( 31)	15.475(114)	0.09	1.812( 28)	91)	0.12	89)	0.09	-	0.09
-	-	-	-	-18.665(	-	-	-16.533(	-	1.860( -26)	-17.860(	-	1.87
1.792( 34)	16.877(115)	0.13	1.900( 33)	90)	0.15	1.786( 26)	88)	0.13	74)	0.15	-	0.15
-13.130(	-	-	-	-13.033(	-	-	-13.414(	-	1.761( -17)	-13.352(	-	1.80
1.774( 18)	41)	0.12	1.770( 18)	41)	0.13	1.763( 14)	32)	0.1	45)	0.11	-	0.11
-12.105(	-	-	-	-12.048(	-	-	-12.204(	-	1.690( -17)	-12.166(	-	1.79
1.687( 17)	39)	0.16	1.684( 17)	40)	0.17	1.690( 13)	31)	0.16	43)	0.16	-	0.16
-13.197(	-	-	-	-12.924(	-	-	-13.206(	-	1.638( -17)	-12.709(	-	1.84
1.691( 31)	91)	0.07	1.668( 28)	79)	0.06	1.681( 24)	68)	0.08	64)	0.07	-	0.07
-	-	-	-	-15.288(	-	-	-14.342(	-	1.678( -22)	-14.362(	-	1.86
1.671( 36)	14.997(115)	0.08	1.705( 32)	94)	0.09	1.679( 27)	87)	0.08	76)	0.09	-	-

Table S12: List of ring critical points (RCP's) found from topological analysis of experimental and theoretical models for MM of (**1**).

Atoms	NORMAL		SHADE		TDS		SHADE +TDS		SP	
	$\rho$ (e Å <sup>-5</sup> ) 3)	$\nabla^2\rho$ (eÅ <sup>-5</sup> ) 3)								
N(2) - C(1) - H(1) -	0.0	0.0	0.0	0.6	0.4	0.6	0.0	0.6	0.0	0.6
O(03) - C(03) -	4	6	5	0	7	0	5	0	40	21
O(04) - H(04)										
N(3) - C(2) - C(5)-	0.1	2.9	0.1	3.0	0.1	3.0	0.1	3.0	0.1	3.6
C(4) - N(4) - C(3)	5	0	7	0	7	0	7	0	36	17
N(1) - C(1) - N(2) -	0.4	8.2	0.4	8.0	0.4	8.0	0.4	8.0	0.3	9.7
C(2) - C(5)	2	0	3	0	4	0	3	0	88	79

Table S13: Atomic charges (e) from multipole refinements and SP calculations for THEO.

Atom	normal	shade	tds	SHADE+ TDS		SP
	$\Omega$	$\Omega$	$\Omega$	$\Omega$	$\Omega$	$\Omega$
O(1)	-1.1116	-1.2904	-1.1079	-1.1824	-1.2117	
O(2)	-1.3278	-1.3814	-1.1913	-1.3139	-1.23627	

N(1)	-1.3712	-1.3285	-1.2108	-1.4195	-1.11839
N(2)	-1.1033	-1.2221	-0.9884	-1.1385	-1.33221
N(3)	-1.1591	-1.2553	-1.2447	-1.3166	-1.25868
N(4)	-1.0912	-1.1635	-1.2216	-1.1926	-1.18605
C(1)	0.5285	0.3824	0.5494	0.5636	1.08202 1
C(2)	0.5853	0.7702	0.7834	0.7948	0.93900 1
C(3)	1.8507	1.8847	1.9033	1.9715	1.86992
C(4)	1.2974	1.3115	1.2899	1.3252	1.44967 1
C(5)	0.3426	0.2829	0.1994	0.2455	0.39954 8
C(6)	0.1279	-0.1257	0.3819	-0.1346	0.42260 8
C(7)	0.3254	-0.8621	0.1924	-0.9188	0.39809 9
H(6A)	0.3238	0.3725	0.1807	0.3104	0.01102 2
H(6B)	0.0674	0.5488	-0.0248	0.4536	0.05720 6
H(6C)	0.0631	0.0671	-0.0026	0.0859	0.05072 2
H(1A)	0.6851	0.5664	0.5759	0.5262	0.48917 8
H(7A)	0.4203	0.5861	0.4234	0.5967	0.02034 8
H(7B)	0.6539	0.9458	0.3936	0.8579	0.05826 5
H(7C)	-0.594	0.5273	-0.1907	0.4574	0.01818 4
H(1)	0.2487	0.3717	0.2322	0.411	0.07701 8
Total	-0.2382	-0.0117	-0.0774	-0.0172	-0.00049

Table S14: Atomic charges (e) from multipole refinements and SP calculations for MA.

Atom	normal	shade	tds	SHADE+ TDS	SP
	$\Omega$	$\Omega$	$\Omega$	$\Omega$	$\Omega$
O(03)					
O(04)	-1.2263	-1.155	-1.2272	-1.1673	-1.20003
O(01)	-1.3048	-1.1449	-1.3168	-1.1594	-1.20017
O(02)	-1.0949	-0.7144	-1.0915	-0.7165	-1.17247
C(01)	1.5263	1.1154	1.5037	1.1208	1.67813 3
C(03)	1.5675	1.4211	1.5354	1.417	1.68171 5

C(02)	0.132	0.0221	0.1638	0.0648	0.00387
H(04)	0.7246	0.647	0.739	0.54777	0.08857
					3
H(01)	0.5852	0.5529	0.59	0.5477	0.59718
H(02A)	0.1277	0.1199	0.1228	0.1058	0.08857
					3
H(02B)	0.0399	0.1097	0.0418	0.1018	0.10403
					8
Total	-0.0245	-0.0086	-0.0272	-0.0046	0.00012

Table 15: Atomic charges (e) from multipole refinements and SP calculations for (1).

	$\Omega$ Normal	$\Omega$ SHADE	$\Omega$ SHADE+TDS	$\Omega$ TDS	$\Omega$ SP
O(2)	-1.0580	-1.0341	-1.0350	-1.0426	-1.1443
O(1)	-1.1362	-1.1083	-1.1028	-1.1178	-1.1329
O(04)	-1.1521	-1.1484	-1.0999	-1.1026	-1.1682
O(03)	-1.1098	-1.0899	-1.1012	-1.1065	-1.1531
O(02)	-1.0704	-1.0468	-1.0387	-1.0447	-1.1303
O(01)	-1.2881	-1.2683	-1.2143	-1.2260	-1.1041
N(4)	-0.9801	-0.9497	-0.9728	-0.9939	-1.1267
N(3)	-1.0826	-1.0526	-1.0766	-1.0980	-1.1550
N(2)	-0.7893	-0.7457	-0.7554	-0.7933	-1.1183
N(1)	0.6759	-1.1838	-1.1463	-1.1655	-1.1763
H(7C)	0.1078	0.0242	0.0239	0.1222	0.0474
H(7B)	0.1721	0.2085	0.2207	0.0660	0.0564
H(7A)	0.0524	0.0085	-0.0004	0.1222	0.0891
H(6C)	0.1567	-0.0511	-0.0354	0.0462	0.0537
H(6B)	0.5876	0.1273	0.1346	0.1498	0.0996
H(6A)	0.5876	0.0548	0.0763	-0.0116	0.0423
H(1A)	0.5876	0.5191	0.5083	0.5615	0.4604
H(1)	0.3206	0.1868	0.2100	0.3027	0.1478
H(04)	0.2887	0.5860	0.5336	0.7148	0.6417
H(02B)	0.1131	0.2417	0.1624	0.2102	0.0841
H(02A)	0.7619	0.1441	0.2083	0.0932	0.0891
H(01)	0.1689	0.7473	0.7156	0.6149	0.5932
C(7)	0.2868	0.4347	0.3419	0.2834	0.3245
C(6)	0.1836	0.2474	0.2629	0.2467	0.3244
C(5)	0.3569	0.3689	0.3005	0.3060	0.3981
C(4)	1.2285	1.2334	1.2454	1.2517	1.3749
C(3)	1.5704	1.5697	1.6280	1.6282	1.6970
C(2)	0.6093	0.6203	0.6023	0.6007	0.8416
C(1)	0.5124	0.5871	0.6219	0.5722	0.9657
C(03)	1.4404	1.4641	1.4611	1.4450	1.5444
C(02)	0.0187	0.0376	-0.0355	0.0003	0.0120
C(01)	1.2897	1.2959	1.3848	1.3838	1.5219

### Hirshfeld Surfaces and fingerprint statistics.

Table S16: Equiprobable surface contacts with in THEO, all values are %.

THEO	H (polar)	C	N	O	H

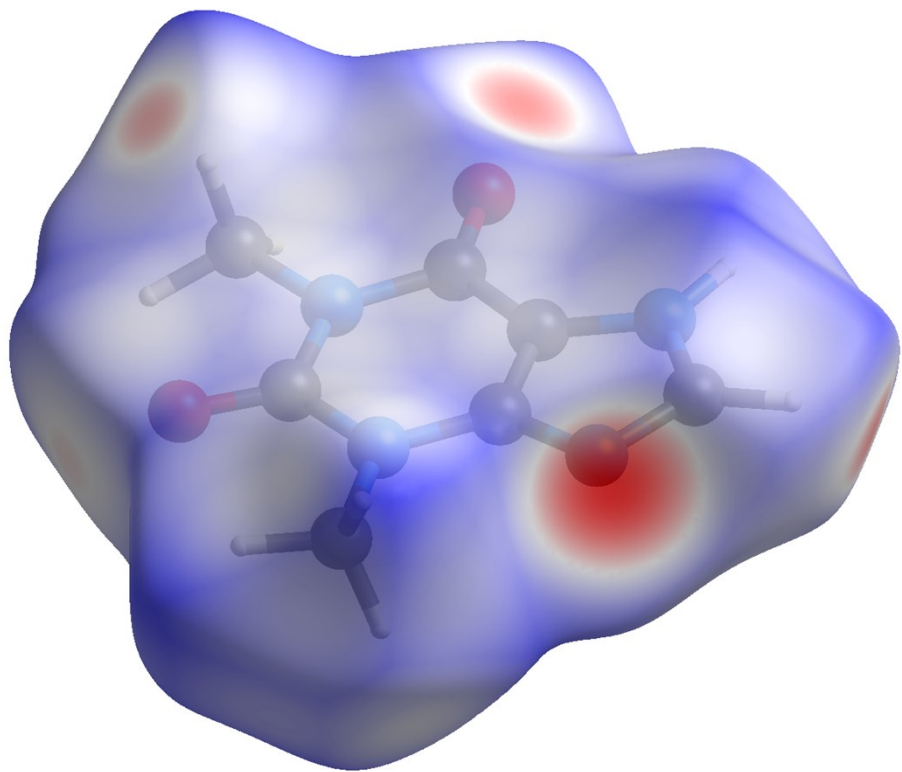
					(hydrophobic)
H (polar)	0.4				
C	3.1	5.96			
N	1.31	5.02	1.06		
O	1.92	7.38	3.11	2.28	
H (hydrophobic)	5.57	21.41	9.01	13.25	19.21

Table S17: Equiprobable surface contacts with in MA, all values are %.

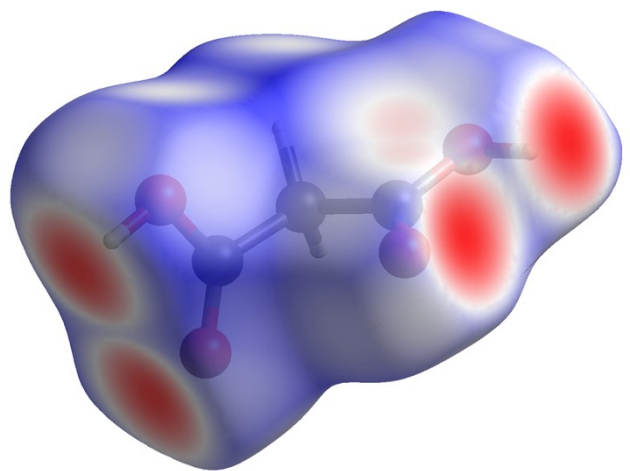
MA	H (polar)	C	O	H (hydrophobic)
H (polar)	3.85			
C	5.06	1.66		
O	18.27	11.96	21.59	
H (hydrophobic)	8.25	5.41	19.53	4.41

Table S18: Equiprobable surface contacts with in (1), all values are %.

THEO	H (hydrophilic)	C	N	O	H(Hydrophobic)
H	1.66				
C	5.88	5.19			
N	1.08	1.92	0.18		
O	7.6	13.42	2.48	8.68	
HC	7.91	13.97	2.58	18.06	9.4
MA	H (hydrophilic)	C	N	O	H(Hydrophobic)
H	1.17				
C	3.64	2.83			
N	2.16	3.36	1		
O	5.03	7.82	4.64	5.4	
HC	8.47	13.16	7.82	18.18	15.31



(a)



(b)

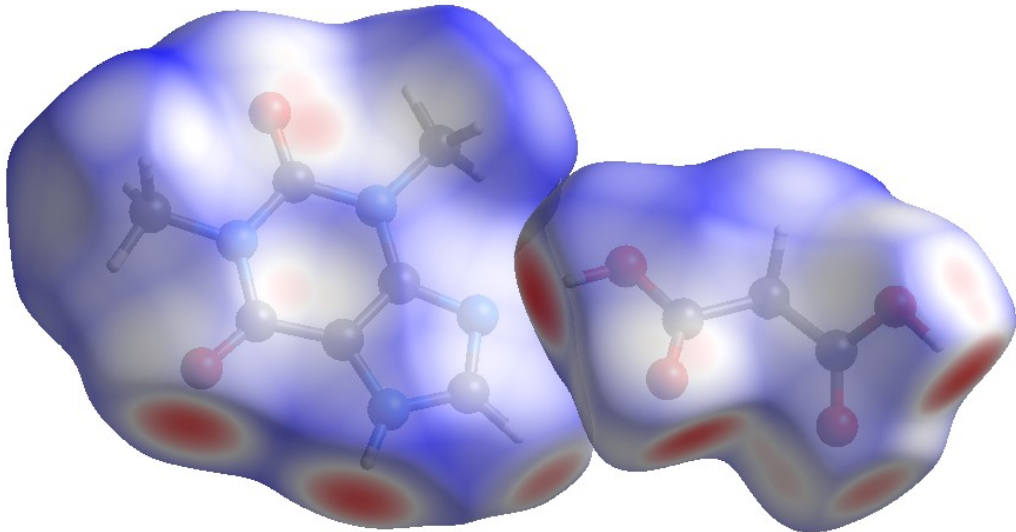


Figure S5: Hirshfeld surface of THEO, MA and (1), a, b and c, respectively

- (1) Trask, A. V.; Motherwell, W. D.; Jones, W., Physical stability enhancement of theophylline via cocrystallization. *Int. J. Pharm.* **2006**, 320, (1-2), 114-23.
- (2) Blessing, R. H., Data reduction and error analysis for accurate single crystal diffraction intensities. *Crystallogr. Rev.* **1987**, 1, (1), 3-58.
- (3) Sheldrick, G. M., A short history of SHELX. *Acta Crystallogr., Sect. A: Found. Crystallogr.* **2008**, 64, (1), 112-122.
- (4) Allen, F. H.; Kennard, O.; Watson, D. G.; Brammer, L.; Orpen, A. G.; Taylor, R., Tables of bond lengths determined by x-ray and neutron diffraction. Part 1. Bond lengths in organic compounds. *J. Chem. Soc., Perkin Trans. 2* **1987**, (12), S1-S19.
- (5) Volkov, A.; Macchi, P.; Farrugia, L. J.; Gatti, C.; Mallinson, P.; Richter, T.; Koritsanszky, T. *XD2006- a computer program for multipole refinement, topological analysis of charge densities and evaluation of intermolecular energies from experimental or theoretical structure factors*, 2006.
- (6) Hirshfeld, F. L., Can x-ray data distinguish bonding effects from vibrational smearing? *Acta Crystallogr., Sect. A* **1976**, A32, Pt. 2, 239-44.
- (7) Tsirelson, V. G.; Ozerov, R. P., *Electron density and bonding in crystals: Principles, theory and X-ray diffraction experiments in solid state physics and chemistry*. ed.; CRC Press: 1996.
- (8) Niepötter, B.; Herbst-Irmer, R.; Stalke, D., Empirical correction for resolution-and temperature-dependent errors caused by factors such as thermal diffuse scattering. *J. Appl. Crystallogr.* **2015**, 48, (5), 1485-1497.
- (9) Meindl, K.; Henn, J., Foundations of residual-density analysis. *Acta Crystallographica A-Foundation and Advances* **2008**, 64, (3), 404-418.
- (10) Madsen, A. O.; Sorensen, H. O.; Flensburg, C.; Stewart, R. F.; Larsen, S., Modeling of the nuclear parameters for H atoms in X-ray charge-density studies. *Acta Crystallogr., Sect. A: Found. Crystallogr.* **2004**, A60, (6), 550-561.

- (11) Madsen, A. O., SHADE web server for estimation of hydrogen anisotropic displacement parameters. *J. Appl. Crystallogr.* **2006**, 39, (5), 757-758.
- (12) Schomaker, V.; Trueblood, K. N., On the rigid-body motion of molecules in crystals. *Acta Crystallographica Section B* **1968**, 24, (1), 63-76.